

Frame and Burst Acquisition in TDMA Satellite Communication Networks with Transponder Hopping

Vitalice K. Oduol and Cemal Ardil

Abstract—The paper presents frame and burst acquisition in a satellite communication network based on time division multiple access (TDMA) in which the transmissions may be carried on different transponders. A unique word pattern is used for the acquisition process. The search for the frame is aided by soft-decision of QPSK modulated signals in an additive white Gaussian channel. Results show that when the false alarm rate is low the probability of detection is also low, and the acquisition time is long. Conversely when the false alarm rate is high, the probability of detection is also high and the acquisition time is short. Thus the system operators can trade high false alarm rates for high detection probabilities and shorter acquisition times.

Keywords—burst acquisition, burst time plan, frame acquisition, satellite access, satellite TDMA, unique word detection

I. INTRODUCTION

THE paper presents the frame and burst acquisition in a satellite communication network consisting of a set of traffic stations (also referred to as terminals) and a master reference station as shown in Fig.1 The access to the satellite resources can be achieved in many ways. Satellite communications multiple access is discussed extensively in several texts [1-6]. In the method of time division multiple access (TDMA) a frame is divided into time slots, which are shared among the terminals. A master station with visibility of the whole network maintains access discipline and scheduling

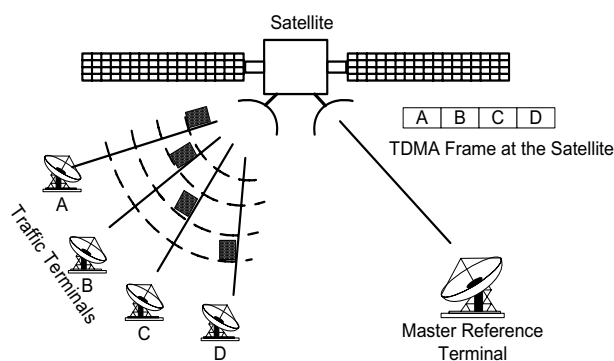


Fig.1 Example TDMA satellite network consisting of traffic terminals and a master reference terminal

during the frame each terminal is allowed to transmit a burst according to a burst transmission plan (BTP). For every transponder the BTP specifies the frequency and polarization

V. K. Oduol is with the Department of Electrical and Information Engineering, University of Nairobi, Nairobi, Kenya (+254-02-318262 ext.28327, vkoduol@uonbi.ac.ke, http://www.uonbi.ac.ke)
 Cemal Ardil is with the National Academy of Aviation, Baku, Azerbaijan .

of the transmissions as well as the position and duration of each burst in the frame; additionally the name or identification of the originating station is indicated. For some networks, such as the INTELSAT system, the BTP also shows the destination station as well as whether as order wires [7]. In the example satellite communication network of Fig.1 there are four traffic terminals that share the satellite resources via TDMA. The terminals transmit their bursts in sequence as shown, with the master reference station maintaining the timing sequence.

For its proper operation TDMA requires synchronization so that the bursts arrive at the satellite in the allotted time slots. The success of synchronization depends on the co-operating stations, reference station, motion of the satellite and estimation methods. In some systems a secondary reference station is used to send timing corrections to communicating station pairs whose mutual bursts are visible from the reference.

Fig.2 shows the frame and burst structure for the TDMA satellite network. Each traffic terminal receives a reference burst from the master station.

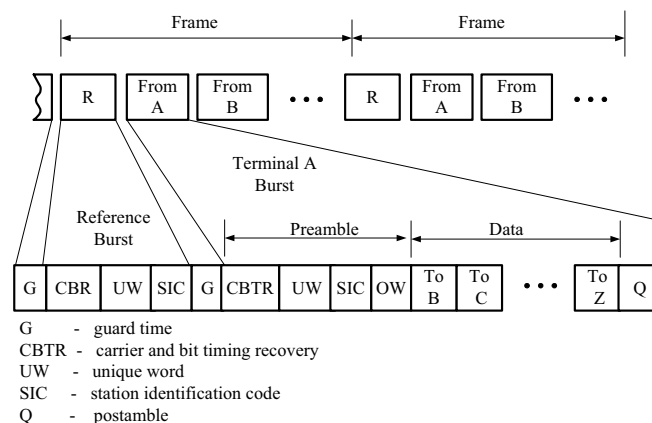


Fig.2 Frame and burst structure for a TDMA satellite network

The reference burst consists of bit patterns for carrier and bit timing recovery (CBTR), the unique word, used to resolve phase ambiguity associated with coherent demodulation, and finally the station identification code (SIC). Timing phase ambiguity may arise due to the carrier and clock recovery method used [2].

The analysis presented in this paper concentrates on the unique word detection at a traffic terminal; it is assumed that carrier recovery and bit timing have been partially

accomplished using the CBTR pattern. Fundamental to the synchronization of any TDMA satellite communication system is the acquisition of the frame.

Transponder Hopping

A single TDMA terminal can extend its capacity by having access to several down link beams by transponder hopping. In one frame the bursts can be sent on different frequencies or different polarizations. That is a terminal is able in one frame to send a burst on one transponder and another burst on another transponder. In such a network each terminal trying to gain acquisition must use the received signals and employ a search strategy that accommodates the many transponders that may be in use.

A typical earth station attempts to gain synchronization from one transponder, and if that fails it tries another one until it succeeds. One advantage of this multi-frequency system is that the transmissions can be achieved at lower peak power [1]. Of course in the frequency domain the TDMA carriers are separated by guard bands.

The rest of the paper is organized as follows. Section II presents the system model in which the acquisition procedure is outlined. It is in this section that the frame acquisition time is derived in terms of the parameters to be obtained later from the modulation and demodulation. Section III presents the QPSK modulation and demodulation and prepares the for the derivation of the detection variable of Section IV. Section V discusses the probability of false alarm. Section VI presents the probability of detection and finally Section VII presents the results and conclusion.

II. SYSTEM MODEL

The unique word search procedure is depicted in Fig.2, which illustrates the case where the traffic terminal expects one of N transponders. For purposes of definiteness the figure is illustrated with N = 8. The labels, k, k+1, ..., k+7, in the circles are given modulo-8. Search procedures are commonly employed in the acquisition of spread spectrum signals are discussed in [8] and more recently in [9] and [10].

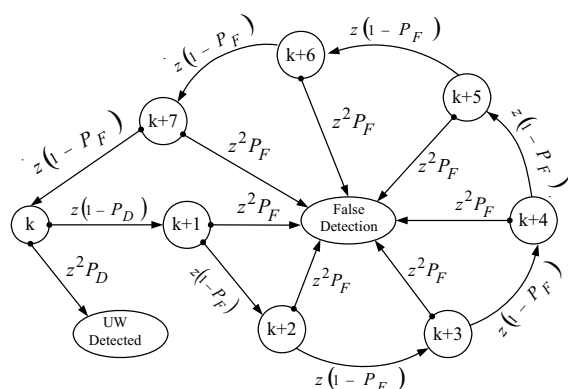


Fig.2 Search procedure for the unique word pattern

The search method used in this paper resembles the serial search method of [11] except that here several frequencies and

polarizations may be used to account for the transponders used. The search can begin in any one of the circles, and it is assumed that the unique word is present at location k (i.e. transponder k).

When the search parameters are for any transponder other than the one in use (k in this case) there can be one of two subsequent events. Either a false detection occurs or the system proceeds to adjust the search parameters for the next transponder. Any detection (false or otherwise) is followed by a verification during the next frame, and therefore consumes two frame times, as is indicated in Fig.2 by the factor z^2 .

When there is no detection the system proceeds to the next frame in one step. This is signified by the factor z. When there is a false detection it is assumed that the verification stage will indicate that there no unique word, and the system will proceed to look over next transponder. Thus in both cases, the receiver proceeds to the next transponder, one case occurring in two frames, while the other takes only one frame.

When the receiver searches over transponder k, it is possible to have detection of the unique word. It is also possible to miss the unique word altogether; in which case the receiver proceeds to the next transponder after one frame. This requires two frames.

Unique Word Acquisition Time

Fig.3 shows the signal flow diagram for the generating function $T_D(z)$ of the time to the acquisition of the unique word pattern. The function $H_0(z)$ in the figure is given by

$$H_0(z) = z^2 P_F + z(1 - P_F) \quad (1)$$

and represents the fact that there are two event paths for proceeding to the next transponder when there is unique word. The first block in the figure signifies the fact the system may start the search q steps from the transponder containing the unique word. Once the transponder with the unique word is reached, the system proceeds in a sequence with a positive feedback.

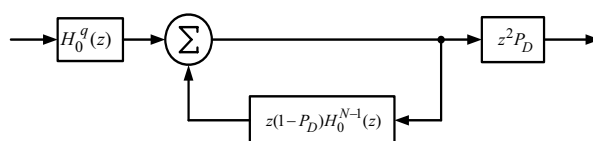


Fig.3 Signal flow for the unique word acquisition time

If the unique word is missed then all the intervening N-1 transponders must be searched before returning to the right one. This explains the role of the block in the feedback path. The block at the right of the figure represents detection, which requires two frames.

Depending on the starting transponder (q steps away), the conditional moment generating function $T_D(z | q)$ is

$$T_D(z | q) = \frac{(z^2 P_D)^q H_0^q(z)}{1 - z(1 - P_D) H_0^{N-1}(z)} \quad (2)$$

When the transponder q is used with probability π_q , then the moment generating function $T_D(z)$ for the acquisition time can be obtained by averaging (2) over q to give

$$T_D(z) = \left(\sum_{q=0}^{N-1} \pi_q H_0^q(z) \right) \frac{z^2 P_D}{1 - z(1 - P_D)H_0^{N-1}(z)} \quad (3)$$

If the transponders are used with equal probability ($\pi_q = 1/N$) then the sum in (3) becomes

$$\sum_{q=0}^{N-1} \pi_q H_0^q(z) = \frac{1}{N} \left(\frac{1 - H_0^N(z)}{1 - H_0(z)} \right) \quad (4)$$

The probabilities P_D and P_F of detection and false alarm, respectively, appearing explicitly or otherwise in (2) and (3) and also in Fig.2 and Fig.3, depend on the modulation and channel type and conditions. The next section discusses how these quantities are determined for a QPSK modulation system that uses a soft-decision approach to the demodulation in an additive Gaussian noise channel. Although the discussion covers expressions that would incorporate timing error, the results given assume perfect timing. Including the effects of timing errors would make the paper too long. The mean acquisition time is then obtained from $T_D(z)$ and taking the derivative of $T_D(z)$ at $z = 1$.

$$\left. \frac{dT_D(z)}{dz} \right|_{z=1} = 1 + \frac{1}{P_D} + \left(\frac{1}{P_D} - 1 \right) (1 + P_F)^{N-1} + (1 + P_F) \sum_{q=0}^{N-1} q \pi_q \quad (5)$$

If the transponders are deployed with equal probability the sum in (5) equals $(N-1)/2$. In that case the mean acquisition time (5) becomes

$$T_{Acq} = 1 + \frac{1}{P_D} + \left(\frac{1}{P_D} - \frac{1}{2} \right) (1 + P_F)^{N-1} \quad (6)$$

Since the probability P_D of detection depends on the probability P_F of false alarm and the signal to noise ratio, the dependence of the acquisition time on the system parameters will be given after the contribution of the modulation and demodulation. These are addressed in the next section.

III. QPSK MODULATION AND DEMODULATION

The QPSK modulator and demodulator used in the TDMA satellite system are shown Fig.4 and Fig.5, respectively. The in-phase and quadrature data streams $a_n^{(I)}$ and $a_n^{(Q)}$ are used as impulse inputs to pulse shaping linear systems of impulse response $h(t)$ and transfer function $H(f)$.

These are then carried on two carriers of the same frequency but in phase quadrature, and summed to produce the transmitted signal, as shown at the bottom of the diagram of Fig.4. On passing through the channel the signal incurs additive white Gaussian noise.

At the receiver the demodulator uses the structure shown in Fig.5. As in Fig.4, two carriers in phase quadrature are used.

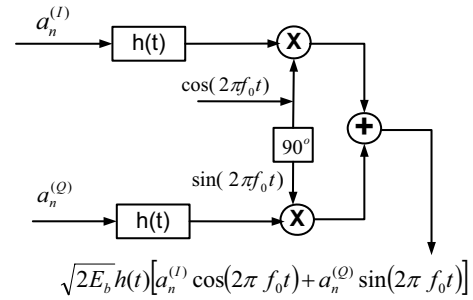


Fig. 4. QPSK Modulator

The figure incorporates an unknown phase ϕ to account for phase differences between the transmitting and receiving carriers. The received signal (excluding the noise term) is given by

$$r(t) = \sqrt{2E_b} h(t) [q_n^{(I)} \cos(2\pi f_0 t) + q_n^{(Q)} \sin(2\pi f_0 t)] \quad (7)$$

The variables $q_n^{(I)}$ and $q_n^{(Q)}$ are used in place of $a_n^{(I)}$ and $a_n^{(Q)}$ to signify the fact that the latter pair could have been altered in transit. In both the I and the Q channels, the received signal is first multiplied by the corresponding carrier signal ($\cos 2\pi f_0 t$ or $\sin 2\pi f_0 t$) and then filtered by a matched filter with impulse response $h_M(t)$ and transfer function is $H_M(f) = H^*(f)$.

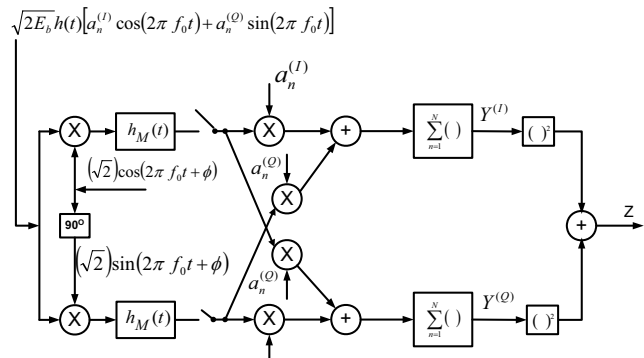


Fig.5 QPSK Demodulator

The resulting signals have double frequency terms, which are removed by the filter, leaving

$$r(t) (\sqrt{2}) \cos 2\pi f_0 t = \sqrt{E_b} h(t) [q_n^{(I)} \cos \phi + q_n^{(Q)} \sin \phi] \quad (8)$$

$$r(t) (\sqrt{2}) \sin 2\pi f_0 t = \sqrt{E_b} h(t) [-q_n^{(I)} \sin \phi + q_n^{(Q)} \cos \phi] \quad (9)$$

The matched filter outputs are sampled at $t = nT + \tau$. This assumes a clock timing offset of τ seconds from the desired instant. Letting $R(\tau)$ be the relative matched filter output, it is assumed in what follows that the sampling is done at $t = \tau$. That is,

$$R(\tau) = 2 \int_0^\infty |H(f)|^2 \cos(2\pi f\tau) df \quad (10)$$

The two options of band-limited and time-limited forms are given in [1] for the pulse-shaping function $H(f)$, resulting in

$$R(\tau) = \begin{cases} 1-|\tau|/T & |\tau| < T \\ 0 & |\tau| \geq T \end{cases} \quad \text{time-limited} \quad (11)$$

$$R(\tau) = \frac{\sin(\pi\tau/T)}{(\pi\tau/T)} \quad \text{band-limited} \quad (12)$$

In addition to (11) and (12), one pulse shape that has gained popularity is the root raised cosine (RRC) pulse which in the frequency domain has the following squared magnitude representation

$$|H(f)|^2 = \begin{cases} 1 & |f| \leq \frac{1-\alpha}{2T} \\ \frac{1}{2} + \frac{1}{2} \cos\left(\frac{\pi T}{\alpha} \left[|f| + \frac{1-\alpha}{2T}\right]\right) & \frac{1-\alpha}{2T} < |f| \leq \frac{1+\alpha}{2T} \\ 0 & |f| > \frac{1+\alpha}{2T} \end{cases} \quad (13)$$

The parameter α is the excess bandwidth, and is restricted to the values $0 \leq \alpha \leq 1$. The relative matched filter response for this pulse shape is the inverse Fourier transform of (13), and is seen to be

$$R(\tau) = \frac{\sin(\pi\alpha\tau/T) \cos(\pi\alpha\tau/T)}{(\pi\alpha\tau/T) 1 - 4\alpha^2\tau^2/T^2} \quad (14)$$

If there is no timing error then the matched filter response is at its peak, i.e. $R(\tau) = 1$.

Returning to the sampled filter outputs, it is observed that the I-channels value is $\frac{1}{2}\sqrt{E_b}R(\tau)[q_n^{(I)} \cos\phi + q_n^{(Q)} \sin\phi]$, while the Q-channel one is $\frac{1}{2}\sqrt{E_b}R(\tau)[q_n^{(Q)} \cos\phi - q_n^{(I)} \sin\phi]$.

These quantities are multiplied by local copies of the unique word pattern and summed, resulting in a correlation values for the I-and Q- channels. From Fig.5, prior to the squaring elements, the I-channel and Q-channel variables are

$$Y^{(I)} = \frac{1}{2}\sqrt{E_b}R(\tau) \cos\phi \sum_{n=1}^N (a_n^{(I)}q_n^{(I)} + a_n^{(I)}q_n^{(I)}) + \frac{1}{2}\sqrt{E_b}R(\tau) \sin\phi \sum_{n=1}^N (a_n^{(I)}q_n^{(Q)} - a_n^{(Q)}q_n^{(I)}) + V^{(I)} \quad (15)$$

$$Y^{(Q)} = \frac{1}{2}\sqrt{E_b}R(\tau) \cos\phi \sum_{n=1}^N (a_n^{(Q)}q_n^{(I)} - a_n^{(I)}q_n^{(Q)}) + \frac{1}{2}\sqrt{E_b}R(\tau) \sin\phi \sum_{n=1}^N (a_n^{(I)}q_n^{(I)} + a_n^{(Q)}q_n^{(Q)}) + V^{(Q)} \quad (16)$$

where the noise terms $V^{(I)}$ and $V^{(Q)}$ are independent and normally distributed, each with zero mean and variance $NN_0/2$. At this point it convenient to define the correlations via the matrix

$$\begin{pmatrix} R_{aq}^{(I)} & R_{aq}^{(IQ)} \\ R_{aq}^{(QI)} & R_{aq}^{(Q)} \end{pmatrix} = \begin{pmatrix} \frac{1}{N} \sum_{n=1}^N a_n^{(I)}q_n^{(I)} & \frac{1}{N} \sum_{n=1}^N a_n^{(I)}q_n^{(Q)} \\ \frac{1}{N} \sum_{n=1}^N a_n^{(Q)}q_n^{(I)} & \frac{1}{N} \sum_{n=1}^N a_n^{(Q)}q_n^{(Q)} \end{pmatrix} \quad (17)$$

and note that in the presence of the unique word, these correlations are found to be

$$R_{aq}^{(I)} = R_{aq}^{(Q)} = 1 \quad (18a)$$

$$R_{aq}^{(IQ)} = R_{aq}^{(QI)} = -1. \quad (18b)$$

In absence of the unique word, these four sums are random variables that are identically distributed, since they are obtained by correlating a random sequence by a known sequence (the unique word). The result is obtained by considering that to get k agreements and $N - k$ disagreements between the known unique word sequence and the random sequence, producing an output of $2k - N$, is equivalent to having k successes in N trials of a Bernoulli process with probability of success $p = 1/2$. Finally the resulting sum is divided by N . Therefore

$$\Pr\left\{R_{aq} = \frac{2k}{N} - 1\right\} = \begin{cases} 2^{-N} \binom{N}{k} & k = 0, 1, 2, \dots, N \\ 0 & \text{otherwise} \end{cases} \quad (19)$$

This can be written in the equivalent form as

$$\Pr\left\{R_{aq} = \frac{2m}{N}\right\} = \begin{cases} 2^{-N} \binom{N}{m + N/2} & m = 0, \pm 1, \pm 2, \dots, \pm \frac{N}{2} \\ 0 & \text{otherwise} \end{cases} \quad (20)$$

Exploiting the obvious symmetry in (20a) and (20b), it is clear that the mean is zero and the mean square is unity. That is, when the unique word is absent, $E\{R_{aq}\} = 0$ and $E\{R_{aq}^2\} = 1$. We can therefore write

$$\begin{aligned} \mu_x &= E\{Y^{(I)}\} = N\sqrt{E_b}R(\tau) \cos\phi \\ \mu_y &= E\{Y^{(Q)}\} = N\sqrt{E_b}R(\tau) \sin\phi \end{aligned} \quad \text{UW present} \quad (21)$$

$$\mu_x = \mu_y = E\{Y^{(I)}\} = E\{Y^{(Q)}\} = 0 \quad \text{UW absent} \quad (22)$$

In the absence of the unique word, the random sequences can be considered as noise, and the analysis can proceed by assuming that the introduced noise is also Gaussian (certainly true if N is large enough). This assumption is necessary for mathematical tractability of the analysis.

Random Sequences as Noise

If the sequences are considered as noise, then total noise in the channel is still Gaussian, with zero mean and variances given by

$$\begin{aligned} \text{Var}\{Y^{(I)}\} &= \text{Var}\{Y^{(Q)}\} = \sigma_0^2 \\ &= \frac{NN_0}{2} + NE_bR^2(\tau)E\{R_{aq}^2\} \end{aligned} \quad (23)$$

Substituting for $E\{R_{aq}^2\}$ gives

$$\sigma_0^2 = \begin{cases} NN_0/2 & \text{UW present} \\ NN_0/2 + NE_bR^2(\tau) & \text{UW absent} \end{cases} \quad (24)$$

IV. THE DETECTION VARIABLE

When the unique word is present the detection variable $Z = [Y^{(I)}]^2 + [Y^{(Q)}]^2$ incorporate the fact that the in-phase and quadrature means are now $E\{Y^{(I)}\} = N\sqrt{E_b}R(\tau)\cos\phi$, and

$E\{Y^{(Q)}\} = N\sqrt{E_b}R(\tau)\sin\phi$. The joint probability density function for the two variables

$$f_{XY}(x, y) = \left(\frac{1}{2\pi\sigma_0^2}\right) \exp\left\{\left(\frac{-1}{2\sigma_0^2}\right)\left[(x - \mu_x)^2 + (y - \mu_y)^2\right]\right\} \quad (25)$$

contains a quadratic term in the exponent which can be expressed in polar form as

$$[x - \mu_x]^2 + [y - \mu_y]^2 = r^2 + N^2 E_b R^2(\tau) - 2NrR(\tau)\sqrt{E_b} \cos(\theta - \phi) \quad (26)$$

In polar form, the joint density function becomes

$$f_{R\theta}(r, \theta) = \frac{r}{\sigma_0^2} \exp\left\{\left(\frac{-1}{2\sigma_0^2}\right)\left(r^2 + N^2 E_b R^2(\tau)\right)\right\} \times \left\{\frac{1}{2\pi} \exp\left\{\left(\frac{1}{2\sigma_0^2}\right)\left(2NrR(\tau)\sqrt{E_b} \cos(\theta - \phi)\right)\right\}\right\} \quad (27)$$

The random phase θ is uniformly distributed in $0 \leq \theta \leq 2\pi$. Therefore, we can obtain marginal density function by averaging over θ

$$f_R(r) = \frac{r}{\sigma_0^2} \exp\left\{\left(\frac{-1}{2\sigma_0^2}\right)\left(r^2 + N^2 E_b R^2(\tau)\right)\right\} I_0\left(\frac{NrR(\tau)\sqrt{E_b}}{\sigma_0^2}\right) \quad (28)$$

where $I_0(x) = \frac{1}{2\pi} \int_{-\pi}^{\pi} \exp(x \cos\theta) d\theta$ is the modified Bessel function of order zero. The detection variable has probability density function $f_Z(z)$ given by

$$f_Z(z) = \frac{1}{2\sigma_0^2} \exp\left\{\left(\frac{-1}{2\sigma_0^2}\right)\left(z + 4N^2 E_b R^2(\tau)\right)\right\} I_0\left(\frac{NR(\tau)\sqrt{zE_b}}{\sigma_0^2}\right) \quad (29)$$

The variance σ_0^2 is given by (24). The next section addresses the case for the absence of the unique word.

V. THE PROBABILITY OF FALSE ALARM

In the absence of the unique word the probability density function for the detection variable $Z = [Y^{(I)}]^2 + [Y^{(Q)}]^2$ is obtained from (29) by setting to zero the terms containing E_b since these are the terms that arise from the means of the in-phase and quadrature components as given in (22). Accordingly the probability density function is given by

$$f_Z(z) = \frac{1}{2\sigma_0^2} \exp(-z/2\sigma_0^2) \quad (30)$$

where from (24) $\sigma_0^2 = NE_b R^2(\tau) + NN_0/2$. The probability of false alarm is then the probability that the detection variable exceeds a set threshold.

$$P_F = \frac{1}{2\sigma_0^2} \int_{\theta}^{\infty} \exp(-z/2\sigma_0^2) dz = e^{-\theta/2\sigma_0^2} \quad (31)$$

The result $P_F = e^{-\theta/2\sigma_0^2}$ can re-written as $\theta = -(2\sigma_0^2)\ln(P_F)$, with σ_0^2 taking the appropriate value in (24). It is possible to determine the probability of detection as a function of the false alarm probability. In preparation for that the following is pertinent.

$$\frac{\theta}{2(NN_0/2)} = -\left[1 + \frac{\gamma}{N} R^2(\tau) + \right] \ln(P_F) \quad (32)$$

where $\gamma = NE_b/(N_0/2)$ is the signal to noise ratio.

VI. THE PROBABILITY OF DETECTION

In the presence of the unique word the detection variable has probability density function given (29). The unique word is missed if the detection variable falls below the threshold θ , otherwise detection occurs. The probability of detection P_D is given by

$$P_D = \frac{1}{2\sigma_0^2} \int_{\theta}^{\infty} \exp\left\{\left(\frac{-1}{2\sigma_0^2}\right)\left(z + N^2 E_b R^2(\tau)\right)\right\} I_0\left(\frac{NR(\tau)\sqrt{zE_b}}{\sigma_0^2}\right) dz \quad (33)$$

Using the series expression for the modified Bessel function $I_0(x)$, we can express the expression for P_D as

$$P_D = \exp(-2\gamma R^2(\tau)) (P_F)^{1+(\gamma/N)R^2(\tau)} \times \sum_{m=0}^{\infty} \frac{(\gamma R^2(\tau))^m}{m!} \sum_{q=0}^m \frac{[(-\ln(P_F))]^{q+1} + (\gamma/N)R^2(\tau)]^q}{q!} \quad (34)$$

VII. RESULTS AND CONCLUSION

One set of results for the probability of detection assumes that there are no timing errors, i.e. that $R(\tau) = R(0) = 1$. Fig.6 shows the variations of the probability of detection for $N = 64$ and different values of the channel signal to noise ratio.

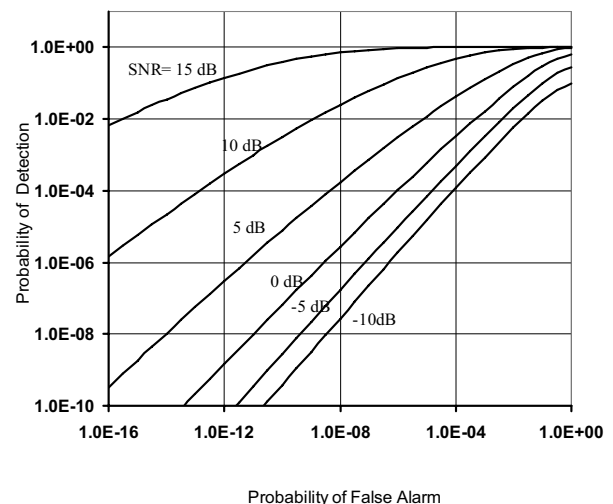


Fig. 6 Variation of the Probability of detection with the signal to noise ratio and false probability

From Fig.6 it is clear that probability of detection increases with the signal to noise ratio, and also with false alarm probability.

Effect of Timing Errors

The presentation given so far allows for a non-zero timing error, i.e. for $R(\tau) < 1$. When timing occur, their effect in the probability of detection as is evident in (34) is to reduce the effective signal to noise ratio. Every occurrence of the signal to noise ratio is multiplied by $R^2(\tau)$. That is the curves in Fig.6 will shift down by an amount equivalent to $R^2(\tau)$ expressed in dB. For example if $R^2(\tau) = 0.64$ the reduction is by about 2 dB. In order to have a clearer interpretation of this it is better to present the detection times and probabilities against the signal to noise ratio with the false alarm probability held temporarily constant.

When the false alarm probability is low (e.g. $P_F = 10^{-8}$ in Fig.7), the probability of detection is low but increases with the signal to noise ratio. When the false alarm probability is high (e.g. $P_F = 0.316$ in Fig.7), the probability of detection is higher and increases with the signal to noise ratio.

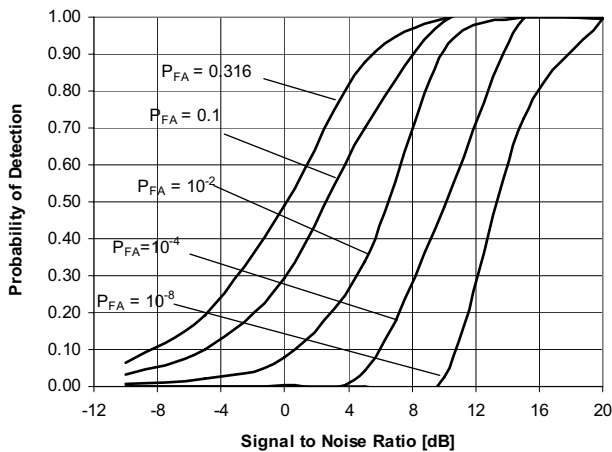


Fig.7 Variation of the probability of detection with signal to noise ratio along curves of constant false alarm rate

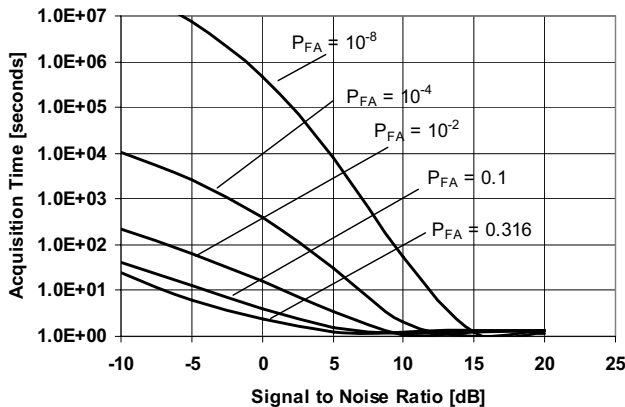


Fig.8 Variation of the acquisition time with signal to noise ratio along curves of constant false alarm rate

Referring to Fig.8, it is seen that when the false alarm probability is low (e.g. $P_F = 10^{-8}$), the acquisition time is long but decreases with the signal to noise ratio, and when the false alarm probability is high (e.g. $P_F = 0.316$), the acquisition time is long shorter and decreases with the signal to noise ratio.

What has emerged here is that high false alarm rate can be tolerated in order to have greater probability of detection and shorter acquisition times. The effect of timing errorson these results is to shift down the curves of Fig.7 (lowering detection probabilities) and shift the curves of Fig.8 (increasing the acquisition time). What was also observed was that as the length N of the unique word was increased, the performance get better.

REFERENCES

- [1] E. Lutz, M. Werner, A. Jahn, *Satellite Systems for Personal and Broadband Communications*, Springer, 2000D.
- [2] Roddy, *Satellite Communications*, 2nd Ed., McGraw-Hill 1996
- [3] G. Maral, M.Bousquet, *Satellite Communications Systems: Systems, Techniques And Technology*, John Wiley & Sons 1999
- [4] J. N. Pelton, *The Basics of Satellite Communications*, 2nd Edition/International Engineering Consortium 2006.
- [5] S. Tirró, *Satellite Communication System Design*, Springer 1993
- [6] M. Richharia, *Satellites Communications Systems*, McGraw-Hill 1999
- [7] D. I. Dalgleish, *An Introduction to Satellite Communications*, Institution of Engineers, IET 1989
- [8] A. J. Viterbi, *CDMA: Principles of Spread Spectrum Communication*, Prentice-Hall, 1995
- [9] S.H.Won, L.Hanzo, "Analysis of Serial Search Based Code Acquisition in Multiple Transmit Antenna Aided DS-CDMA Downlink" In: *IEEE VTC'05 (Fall)*, 25-28 September 2005, Intercontinental Hotel, Dallas, Texas, USA.
- [10] H.Puska, H.Saarnisaari, J.Iinatti, P.Lilja, "Serial search code acquisition using smart antennas with single correlator or matched filter", *IEEE Transactions on Communications*, Vol.:56, No.2 pp. 299-308, Feb.2008
- [11] S.Glisic, B. Vucetic, *Spread Spectrum CDMA Systems For Wireless Communications*, Artech House 1997

Vitalice K. Oduol received his pre-university education at Alliance High School in Kenya. In 1981 he was awarded a CIDA scholarship to study electrical engineering at McGill University, Canada, where he received the B.Eng. (Hons.) and M.Eng. degrees in 1985 and 1987, respectively, both in electrical engineering. In June 1992, he received the Ph.D. degree in electrical engineering at McGill University.

He was a research associate and teaching assistant while a graduate student at McGill University. He joined MPB Technologies, Inc. in 1989, where he participated in a variety of projects, including meteor burst communication systems, satellite on-board processing, low probability of intercept radio, among others. In 1994 he joined INTELSAT where he initiated research and development work on the integration of terrestrial wireless and satellite systems. After working at COMSAT Labs. (1996-1997) on VSAT networks, and TranSwitch Corp.(1998-2002) on product definition and architecture, he returned to Kenya, where since 2003 he has been with Department of Electrical and Information Engineering, University of Nairobi.

Dr. Oduol was a two-time recipient of the Douglas tutorial scholarship at McGill University. He is currently chairman, Department of Electrical and Information Engineering, University of Nairobi. His research interests include performance analysis, modeling and simulation of telecommunication systems, adaptive error control, feedback communication.

Cemal Ardil is with the National Academy of Aviation, Baku, Azerbaijan